Desalination and Water Treatment
www.deswater.com
doi: 10.1080/19443994.2015.1043956

57 (2016) 11291–11299
May

Taylor & Francis
Taylor & Francis Group

Removal of phosphate in aqueous solutions by the aluminum salt slag derived from the scrap aluminum melting process

Xianyou Ren[a], Chao Du[a,b], Liang Zhang[a,*], Yanhua Zhuang[a], Meng Xu[a,b]

[a]*Key Laboratory for Environment and Disaster Monitoring and Evaluation, Hubei, Institute of Geodesy and Geophysics, Chinese Academy of Sciences, 340 Xudong Road, Wuhan 430077, China, Tel. +86 27 68881362; emails: rxy@whigg.ac.cn (X. Ren), cdu@whigg.ac.cn (C. Du); Tel. +86 27 68881396; Fax: +86 27 68881362; email: lzhang@whigg.ac.cn (L. Zhang), Tel. +86 27 68881075; email: zhuang@whigg.ac.cn (Y. Zhuang), Tel. +86 27 68881362; email: dream0131@whigg.ac.cn (M. Xu)*
[b]*University of Chinese Academy of Sciences, 19 Yuquan Road, Beijing 100049, China*

Received 17 December 2014; Accepted 16 April 2015

ABSTRACT

Aluminum salt slag, a kind of industrial by-product derived from the scrap aluminum melting process, was used to remove phosphate (P) from aqueous solutions in this research. The morphology and microstructure of the sample was characterized by Brunauer–Emmett–Teller (BET) analysis, X-ray photo-electron spectroscopy, scanning electron microscopy, and X-ray diffraction. According to the results, aluminum salt slag exhibited a surface area of 16.73 m^2/g and a rough surface with many slit-shaped pores, and its main constituents were determined to be aluminum compounds and salt-flux mixture. The experimental kinetic data were well fitted using both the pseudo-second-order model and Elovich model, which revealed its nature of chemisorption and heterogeneous composites. Furthermore, the isotherm studies showed that it followed Freundlich model better than the Langmuir model, the maximal adsorption capacities calculated by Langmuir model were 2.312–3.467 mg/g. The thermodynamics study demonstrated that the adsorption process was endothermic. Additionally, it was found that a pH of 8.0 was most unfavorable to P removal and ligand exchange may be one of the main adsorption mechanisms. With the advantages of huge production, low costs, and desirable treatment efficiency, the aluminum salt slag is proposed to be another possible adsorbent for P removal from wastewater.

Keywords: Aluminum salt slag; Phosphate; Adsorption isotherm; Kinetics; Ligand exchange

1. Introduction

Eutrophication is widely recognized as one of the main environmental problems nowadays, which is associated with the deterioration of water quality [1]. The excessive supply of phosphate (P) is regarded as the main culprit of the eutrophication in water bodies [1,2]. It is necessary to develop effective and safety technologies to remove P from aqueous solutions for water quality improvement.

Related studies during the past decades have explored several typical removing methods, such as chemical precipitation [3], biological treatments [4], electrodialysis [5], ion exchange [6], and adsorption [7]. However, increasing emphasis has been placed on adsorptive removing method considering its easily handle operation, high efficiency, and lower cost [8].

*Corresponding author.

The search for efficient and low-cost materials using for P adsorption removal has been a key issue for more than a decade and the most commonly used adsorbents can be broadly categorized as natural materials, synthetic materials and industrial by-products. Though the natural materials are easily available, most of them have limited adsorption capacities for P removal, such as the apatite [9], the limestone [10], and the peat [11]. By contrast, the synthetic materials are almost all efficient absorbents, but the complicated synthesis technology and high cost are not favor of their wide application. At the same time, some industrial by-products are chosen as adsorption materials and showed great advantage, such as the fly ash [12], the blast furnace slag [13], and iron oxide tailings [14]. Most of these waste materials are easily available and low cost. They are selected as the adsorbents of P, which is not only beneficial to P removal from water bodies, but more conducive to the properly disposing of these wastes themselves, thus minimizing the threat to the ecosystem. As one of the main waste materials in industrial production, the aluminum salt slag derived from scrap aluminum melting process has not been received adequate attention as a novel adsorbent of P in the previous studies.

The aluminum salt slag is a kind of industrial by-product formed during the secondary aluminum production, which is one of the two main routes for aluminum production. In comparison with the another route, production of primary aluminum, the secondary aluminum needs little energy and saves raw materials, as the waste product can be recycled instead of being sent to landfill [15]. Typical sources of aluminum scrap used in secondary aluminum production are process scrap, used beverage cans, foils, extrusions, commercial scraps, turnings, and old rolled or cast metal [16]. In 2010, the total aluminum production was close to 56 million tonnes, among which close to 18 million tonnes were recycled from scrap [17]. This number will definitely increase in the future. The concomitant production of aluminum salt slag in the scrap melting process should not be underestimated. Moreover, the disposal of aluminum salt slag is a worldwide problem. Improper disposal such as landfill without any treatment would cause acute pollution and is forbidden in most countries. As the aluminum salt slag still contains some metals (Al, Mg, and Fe) [18], it was found that the metals contained in some low-cost adsorbents played an important role for their capacity for P removal [19]. This drove us to choose the aluminum salt slag as the P adsorption material in this research. Furthermore, an in-depth understanding of the mechanisms and characteristics of P adsorption by the aluminum salt slag is crucial to its effective utilization as an adsorbent material.

The aim of this study was to evaluate the feasibility of using aluminum salt slag derived from the scrap aluminum melting process as adsorbent for the P removal. The laboratory adsorption batch experiments, the mathematical models of kinetics, and isotherms fitted by both linear and non-linear regression methods, and some characterization methods are used to determine the characteristics of P adsorption. The influences of temperature and solution pH on P removal are also studied.

2. Materials and methods

2.1. Materials

The aluminum salt slag, a by-product formed during aluminum scraps melting process, was used in this research. It generated from a secondly aluminum manufactory at Yueyang city in Hunan province, China.

All reagents were of analytical grade. Artificial wastewater was synthesized by dissolving preweighed potassium dihydrogen phosphate (KH_2PO_4) in deionized water. Artificial P solutions were used throughout the adsorption tests. The pH of the solution was adjusted with 1 M HCl and 1 M NaOH solutions before adsorption experiments.

2.2. Characterization methods

Elemental analyses of the aluminum salt slag were carried out using X-ray fluorescence (XRF) spectrometer (S4 Pioneer, Bruker, Germany). The surface structural properties were analyzed by X-ray photoelectron spectroscopy (XPS) (Escalab 250 xi, Thermo Fisher, America), using a monochromatized Al kα X-ray as the excitation source and choosing C 1s (284.5 eV) as the reference line. The Brunauer–Emmett–Teller (BET) surface area of the aluminum salt slag was analyzed by nitrogen adsorption and desorption method in the adsorption apparatus (ASAP 2020, Micromeritics, U.S.). The BET surface area was determined by a multipoint BET method using the adsorption data in the relative pressure (P/P_0) range of 0.05–1.0. A desorption isotherm was used to determine the pore size distribution by the Barret–Joyner–Halender (BJH) method. The X-ray diffraction (XRD) patterns were obtained on an X-ray diffractometer (X'Pert Pro, PANalytical, Netherlands) using Cu kα radiation at a scan rate of 0.05° 2θ s^{-1} to determine the phase structures of the obtained sample. The samples were

analyzed using a scanning electron microscope (SEM) with an energy dispersive X-ray spectrometer (EDX, Quanta 200, FEI, Netherlands). The pH control measurement (PB-10, Sartorius) was used in adsorption batch experiments.

2.3. Batch adsorption experiments

P adsorption kinetic study was carried out by adding a certain amount of adsorbent (0.5 g) to a 150-mL conical flask filled with 50 mL P solution (50 mg/L). The pH value of the solution was maintained at 7.0 by adding 0.1 M HCl and 0.1 M NaOH solutions. The conical flask was shaken at a constant speed of 170 rpm in a shaking water bath at temperature of 298 K. The samples were taken at different time intervals and immediately filtered with a 0.45-μm polycarbonate filter membrane. The concentrations of P in the solutions were determined spectrophotometrically by the molybdenum blue method, monitoring the absorbance at 700 nm on UV–vis spectrophotometer. The amount of P adsorbed on sample at time t, q_t (mg/g), was calculated by the following equation:

$$q_t = \frac{(C_0 - C_t)V}{W} \quad (1)$$

where C_0 and C_t (mg/L) are the concentrations of P at initial and time t, respectively. V is the volume of the solution (L) and W is the mass of adsorbent used (g).

In the adsorption isotherm study, 2 g adsorbent was added into a series of 150-mL conical flask filled with 50-mL diluted P solutions with different initial concentrations (10–300 mg/L) at pH of 7.0. Samples were taken after 24 h of contact and filtered with a 0.45-μm polycarbonate filter membrane. Moreover, in order to test the effects of temperature, the same procedure should be conducted at three temperatures (288, 298, and 308 K). The amount of P at equilibrium q_e (mg/g) on the adsorbent samples was calculated by the following equation:

$$q_e = \frac{(C_0 - C_e)V}{W} \quad (2)$$

where C_0 and C_e (mg/L) are the liquid phase concentrations of P at initial and equilibrium, respectively, V is the volume of the solution (L) and W is the mass of adsorbent used (g).

In order to test the effects of pH, 50 mL of 200 mg/L P solutions at various initial pHs (3.0–12.0) was prepared in 150-mL conical flasks. The solutions were measured and adjusted accordingly during the experiments by 0.1 M HCl and 0.1 M NaOH solutions. Other procedures were the same as those in the above isotherm experiments.

3. Results and discussion

3.1. Characterization of adsorbents

3.1.1. Chemical composition

The chemical composition of aluminum salt slag depends mainly on the quality of aluminum scrap processed, the operating conditions and the type of technology and furnace applied for Al-metal production [20]. The XRF analysis showed that the as-received aluminum salt slag is mainly composed of aluminum (43.6%), soluble salts (of Na, K, and Cl), and scraps alloying elements (Si, Mg, Fe, Cu, Ti, Zn, Mn, etc.). To reveal the chemical status of aluminum, the detailed XPS spectra of the Al 2p core level was studied. The spectra are presented in Fig. 1. The presence of Al 2p peak at 74.2 ± 0.1 eV demonstrated the chemical bonding of Al_2O_3 gamma and AlOOH beta diaspore.

3.1.2. Specific surface areas and porosity

The typical nitrogen adsorption–desorption isotherms and their corresponding pore size distributions (PSD) curves are usually used to explore the surface area and porosity. It is observed that aluminum salt slag sample displays type IV isotherms. At low relative pressure ($P/P_0 < 0.4$), the dominating process is the formation of a monolayer of adsorbed molecules. At high relative pressure ($P/P_0 > 0.4$), the adsorption

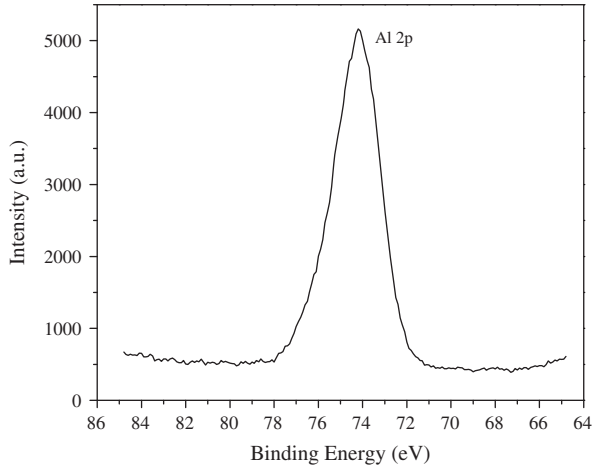

Fig. 1. XPS spectra of Al 2p core level of aluminum salt slag.

in mesopores leads to multilayer formation until condensation takes place. And a H3-type hysteresis loop is observed at high relative pressure between 0.4 and 1.0, which is associated with slit-like pores [21]. This kind of hysteresis loop is usually found on solid consisting of aggregates or agglomerates of particles forming slit-shaped pores (plates or edged particles like cubes) with non-uniform size or shape [22]. The PSD curve of aluminum salt slag sample is quite broad with small mesopores (peak pore at ca. 3.8 nm) and larger ones (peak pore at ca. 10.8 nm). The smaller mesopores reflect pores present within nanosheets, and larger mesopores indicate the pores formed between stacked nanosheets [23]. S_{BET} and $D_{average}$ of the as-received aluminum salt slag are determined to be 16.73 m^2/g and 21.12 nm, respectively. Generally, for adsorbent, a large surface area can offer more active adsorption sites and is advantageous for high adsorption capacities [24].

3.1.3. XRD and SEM analysis

The XRD spectrum of the as-received aluminum salt slag is shown in Fig. 2. It shows that peaks are complex in spectrum and some of them overlapped. Several major and minor phases are identified as $MgAl_2O_4$, Al_2O_3, $MgFeAlO_4$, NaCl, Al_5O_6N, CaF_2, $Cu_{1.4}Mn_{1.6}O_4$, and so on by comparative analysis. First, Al_2O_3 is certainly the result of the reaction of the oxygen with metallic aluminum in the melting process. Then, the appearance of $MgAl_2O_4$, $MgFeAlO_4$, and $Cu_{1.4}Mn_{1.6}O_4$ may be caused by the oxidation reactions of Mg, Fe, Cu, and Mn present in the aluminum scrap as alloying elements [25]. And NaCl and CaF_2 were likely from the molten salt flux, which had been used during the melting process to protect the metal from the reactive atmosphere [26].

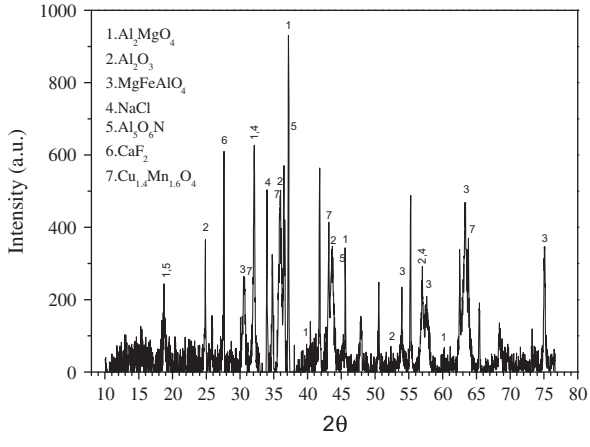

Fig. 2. XRD pattern of the as-received aluminum salt slag.

The aluminum salt slag sample surface before and after P removal experiments was examined by SEM and EDX analyses. Fig. 3 presents the morphology and surface elements distribution of the aluminum salt slag sample examined by SEM/EDX. It shows that the adsorbent consists of many small particles with different morphologies and sizes, resulting in a rough surface and a porous structure (Fig. 3(a) and (b)). And through closer observation and comparison, we found the aluminum salt slag surface after P removal experiment seemed coarser than the original aluminum salt slag surface. It seemed that many small particles were covered in the surface of aluminum salt slag after P removal experiment (Fig. 3(d) and (e)). These small particles were very likely the new precipitations formed in reactions. It is known that the most common method to precipitate P involves the dissolved cations such as Al^{3+}, Ca^{2+}, and Mg^{2+} in water treatment. The EDX analyses demonstrated that the crystalline layer consisted predominantly of Al, O, Si, Mg, and Ca (Fig. 3(c)), whose content changed after P removal experiment. And the peak corresponding to P also appeared after reaction (Fig. 3(f)), though its peak intensity was not particularly high. This demonstrated that precipitation has effect on P adsorption, but it played only a marginal role in the P removal process.

3.2. Phosphate adsorption kinetics

The adsorption kinetics is meaningful to investigating the potential rate-controlling step of adsorption process and to providing valuable data for understanding the mechanism of adsorption reactions [27]. In this research, in addition to the commonly used pseudo-first-order and pseudo-second-order models, the Elovich model was also tested. These models are represented by the following equations [28,29]:

$$\frac{dq_t}{dt} = k_1(q_e - q_t) \quad \text{pseudo-first order} \tag{3}$$

$$\frac{dq_t}{dt} = k_2(q_e - q_t)^2 \quad \text{pseudo-second order} \tag{4}$$

$$\frac{dq_t}{dt} = \alpha \exp(-\beta q_t) \quad \text{Elovich} \tag{5}$$

where t is the contact time of adsorption experiment (h); q_t and q_e are the amount of P adsorbed at time t and at equilibrium, respectively (mg/g); k_1 (L/h) and k_2 (g/mg h) are the pseudo-first-order and pseudo-second-order adsorption rate constants, respectively.

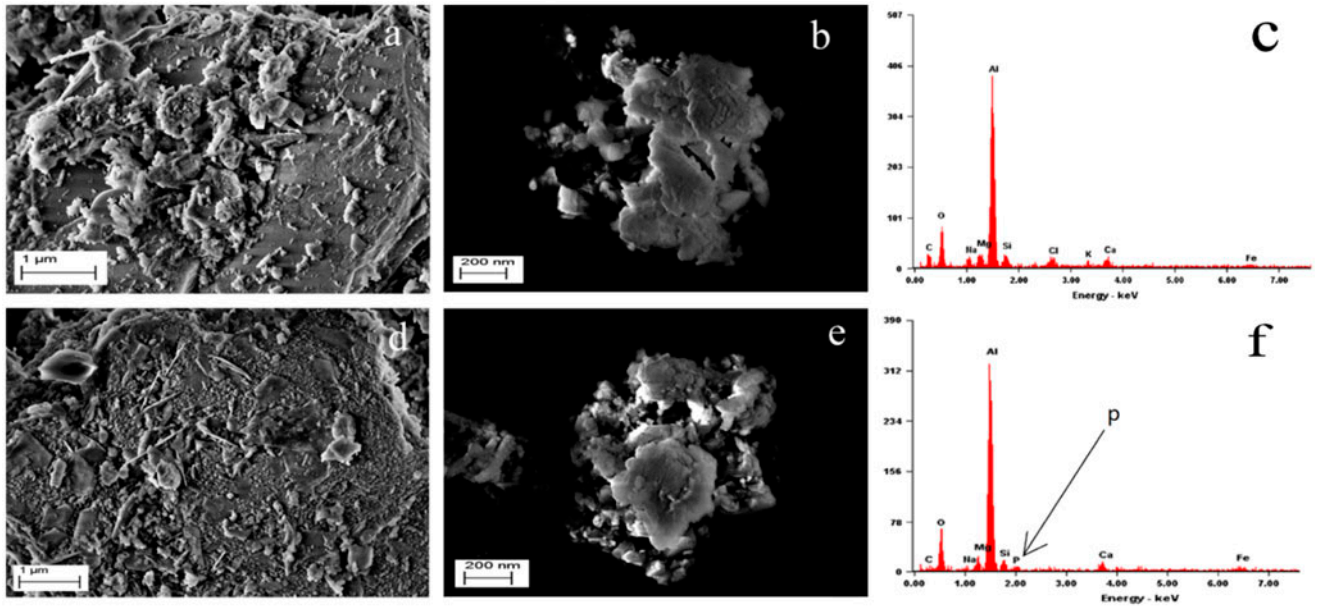

Fig. 3. The SEM–EDX results of aluminum salt slag before and after adsorption of P. (a and b) Surface of aluminum salt slag before P removal; (c) chemical analysis of the surface of aluminum salt slag before P removal; (d and e) surface of aluminum salt slag after P removal; (f) chemical analysis of the surface of aluminum salt slag after P removal.

Also, α is the initial adsorption rate (mg/g h) and β is the desorption constant (g/mg). The pseudo-first-order and pseudo-second-order models describe the kinetics of the solid–solution system based on mononuclear and binuclear, respectively, while the Elovich model is an empirical equation [28].

Fig. 4 shows the experimental data of adsorption kinetics of P onto aluminum salt slag sample. It can be seen that the removal of P from aqueous solutions by adsorption on aluminum salt slag increases with time till the equilibrium is attained. The P removal efficiency was rapid initially and then slowed down gradually until it attained equilibrium. Almost half of P was adsorbed in the first 2 h.

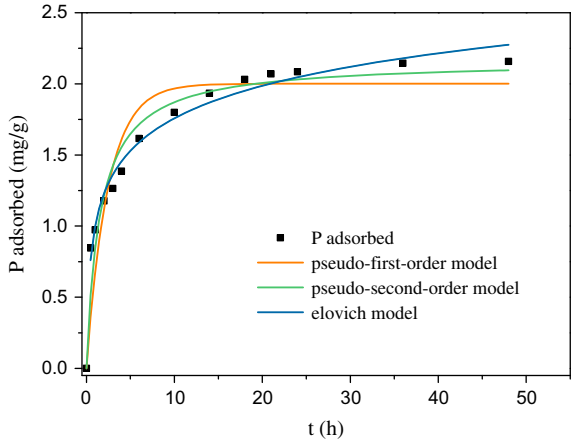

Fig. 4. Kinetics for the adsorption of P onto aluminum salt slag obtained using non-linear regression method.

All the models closely reproduced the kinetic data with all determination coefficients (R^2) exceeding 0.90 (Table 1). Fig. 4 shows the three kinetic models fitting results by non-linear methods. However, the pseudo-second-order model and the Elovich model fitted the data better than the pseudo-first-order model by comparing the R^2 values.

The R^2 values obtained by the pseudo-first-order model are relatively low both by linear and non-linear regression methods. The high applicability (R^2 = 0.957/0.999) of the pseudo-second-order model for the present kinetic data demonstrates that the P adsorption onto aluminum salt slag is chemisorption considering that a pseudo-second-order equation is in agreement with a chemisorption mechanism being the rate-controlling step [29]. Moreover, the fitting of Elovich model was also good (R^2 = 0.977/0.988). This model has been reported to be suitable for highly heterogeneous systems [29]. Taking into account the complex components of aluminum salt slag examined by XRF and XRD, it can be inferred that the powerful activation energy for chemisorption on the surface of aluminum salt slag is generated, which is advantageous to the enhancement of adsorption capacity. The parameters obtained by linear least squares regression

Table 1
Parameters of pseudo-first order, pseudo-second-order, and Elovich models using the linear and non-linear regression methods for the removal of P by aluminum salt slag

	Pseudo-first-order			Pseudo-second-order			Elovich		
Regression methods	k_1 (L/h)	q_e (mg/g)	R^2	k_2 (g/mg h)	q_e (mg/g)	R^2	α (mg/g h)	β (g/mg)	R^2
Linear	0.079	1.014	0.931	0.234	2.243	0.999	6.805	3.032	0.977
Non-linear	0.409	2.000	0.901	0.295	2.164	0.957	6.805	3.032	0.988

method and trial-and-error non-linear regression method are different (Table 1). This may be caused by that the transformations of the non-linear kinetics to the linear forms implicitly altered the error structure [30].

3.3. Adsorption isotherm

Adsorption isotherm was used to estimate P distribution between solid and aqueous phases as a function of adsorbed concentration. Fig. 5 illustrated the adsorption capacities of P onto aluminum salt slag at various temperatures. Obviously, the elevated temperatures favored the P adsorption by aluminum salt slag. The adsorption isotherm data were fitted by two commonly used equilibrium models, Langmuir model (6) and Freundlich model (7) [28]:

$$\frac{C_e}{q_e} = \frac{C_e}{q_{max}} + \frac{1}{K_L q_{max}} \tag{6}$$

$$\log\ q_e = \log K_F + \frac{1}{n}\log\ C_e \tag{7}$$

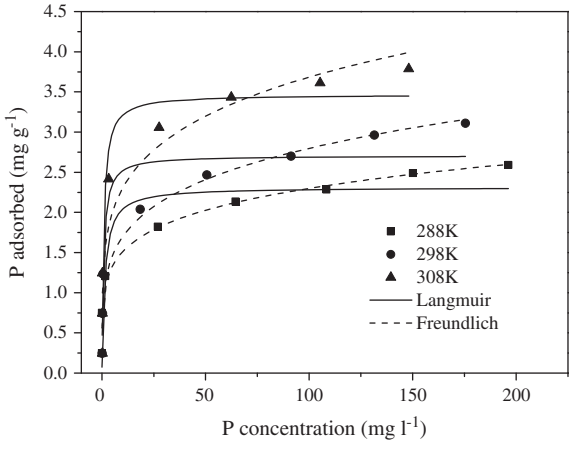

Fig. 5. Adsorption isotherms of P onto aluminum salt slag at various temperatures.

where C_e is the P concentration in the solution (mg/L), q_e is the amount of P adsorbed at equilibrium (mg/g), and q_{max} is the theoretical maximum adsorption capacity (mg/g). K_L represents the Langmuir bonding term related to interaction energies (L/mg), K_F is the Freundlich affinity coefficient ($mg^{(1-n)}\ L^n/kg$) and n is the Freundlich linearity constant.

Table 2 summarizes the parameters of Langmuir and Freundlich isotherms for the P adsorption onto aluminum salt slag at different temperatures. It can be observed that Freundlich equation gives more satisfactory fitting to the adsorption data of P on aluminum salt slag sample with higher R^2 values. Considering that Langmuir model is mainly suitable for monolayer adsorption on smooth and homogeneous surface and Freundlich model is mainly suitable for adsorption on surface with non-uniform energy distribution [31], the results here indicate the possible heterogeneity of surface and formation of multilayer coverage of P molecule on the outer surface of aluminum salt slag. Moreover, the values of q_{max} and K_F increased with temperature increasing which demonstrated that the adsorption process was endothermic in nature. Taking into account the low price and the good adsorption capacity of aluminum salt slag, there is great potential for aluminum salt slag to become an efficient P removal material.

3.4. Adsorption thermodynamics

Thermodynamic parameters can provide useful information about the adsorption process. They can be used to indicate whether the process is spontaneous or not. The thermodynamic equilibrium constants (K_d) were computed using the method of plotting ln (q_e/C_e) vs. q_e and extrapolating q_e to zero under different temperatures as shown in Eq. (8) [32]:

$$K_d = \lim_{q_e \to 0} \ln \frac{q_e}{C_e} \tag{8}$$

In this research, the systems were evaluated by calculating the values of variation of Gibbs free

Table 2
Adsorption isotherm parameters of aluminum salt slag at different temperatures

	Langmuir isotherm model			Freundlich isotherm model		
Temp. (K)	K_L (L/mg)	q_{max} (mg/g)	R^2	n	K_F (mg$^{(1-n)}$ L^n/kg)	R^2
288	0.746	2.312	0.827	5.492	0.994	0.964
298	1.338	2.707	0.899	4.627	1.034	0.950
308	1.245	3.467	0.925	4.899	1.439	0.902

energies (ΔG) obtained at different temperatures. The enthalpy change (ΔH) and entropy change (ΔS) can also be determined by the following equations [33]:

$$\Delta G = -RT \ln K_d \quad (9)$$

$$\ln K_d = \frac{\Delta S}{R} - \frac{\Delta H}{RT} \quad (10)$$

where R (8.314 J/mol/K) is the gas constant, T (K) is the absolute temperature, and K_d is the thermodynamic equilibrium constant. The results of ΔG, ΔH, and ΔS are shown in Fig. 6.

The negative values of ΔG were found at all of the studied temperatures, which confirmed that the adsorption process was spontaneous. Furthermore, the positive values of ΔH suggested that adsorption was carried out as an endothermic process at 288–308 K, i.e. an increase in temperature favored adsorption. Additionally, the positive ΔS value indicated the randomness at the solid–solution interface increased during adsorption [34]. The decrease in ΔG with the increase in temperature showed an increase in feasibility of adsorption at higher temperature [35].

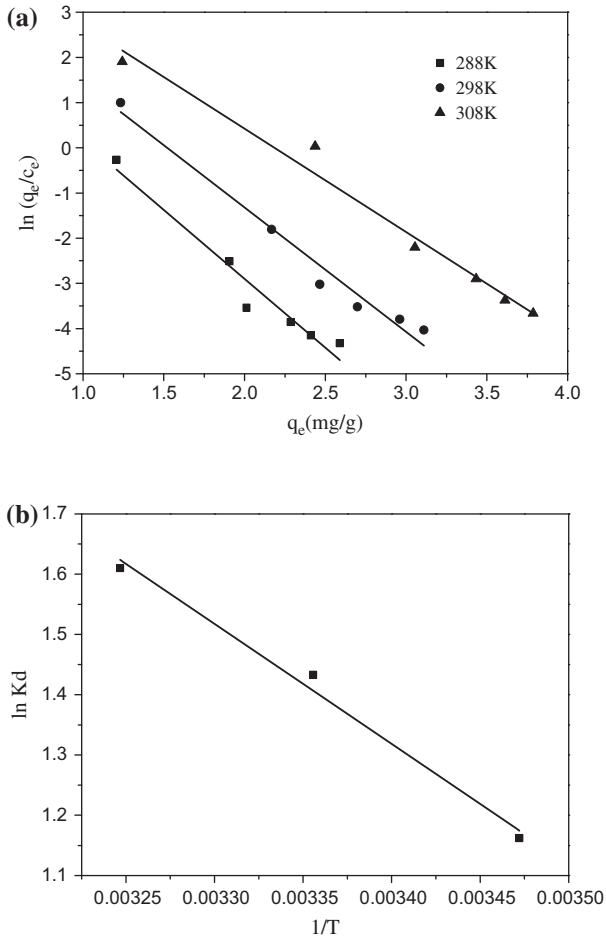

Fig. 6. Adsorption thermodynamics of P adsorption onto aluminum salt slag at different temperatures: (a) plotting ln (q_e/C_e) vs. q_e, (b) plotting ln K_d vs. $1/T$.

3.5. Effects of pH on phosphate adsorption

The pH of a solution generally plays an important role in the physicochemical reaction at the water–solid interface. Fig. 7 demonstrates that the adsorption capacity of aluminum salt slag onto P is strongly dependent on solution pH. The increased pH is a sign of the release of OH^- and consume of H^+. It can be seen that the P adsorption capacity decreased from pH 3.0 to about pH 8.0 and then increased up to pH 12.0. It has been reported that P adsorption on adsorbents is determined by the surface characteristics (especially surface charge) and the protonation state of P in aqueous solution. And the P species are mainly HPO_4^{2-} and $H_2PO_4^-$ with negative charge at the pH range of 2.0–8.0 according to former research [36]. The surface charge of the aluminum salt slag should also be negative at this pH range, which may lead to the electrostatic repulsion between negatively charged adsorbents and P anions. Moreover, the increasing –OH in solution competes strongly with P for active sites while pH rising from 3.0 to 8.0, which affects the adsorption capacity. The two reasons above may result in the decreasing adsorption capacity of P at the pH range of 3.0–8.0. However, the adsorption capacity of P onto aluminum salt slag turned to increase at the pH range

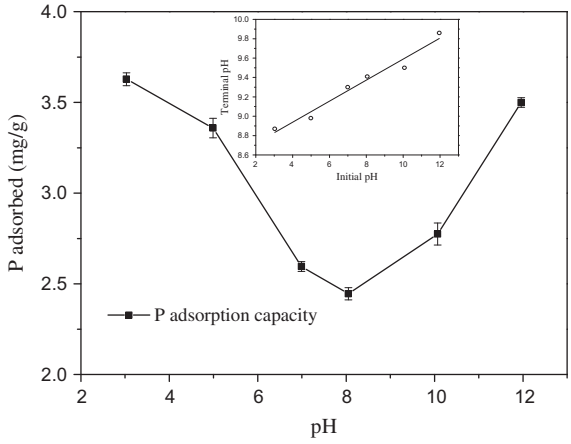

Fig. 7. Effect of pH on P adsorption by aluminum salt slag.

of 8.0–12.0. This indicates that P is adsorbed by the ligand exchange between P (in solution) and –OH (on the surface of aluminum salt slag) at high pH. The aluminum salt slag in this study contains much metallic oxide such as aluminum, ferric, and magnesium oxides with tetrahedral mineral composition [37]. The –OH would bond with these tetrahedrons when Me–O bonds had been cut at high pH. And then the ligand of –OH would be replaced by the HPO_4^{2-} or $H_2PO_4^-$ in aqueous solution, which leads to the increasing of adsorption capacity.

The pH studies demonstrated that one of the major mechanisms for P adsorption process may be described as:

$$2 \equiv Me - OH + H_2PO_4^- \Longleftrightarrow (\equiv Me)_2HPO_4 + H_2O + OH^- \quad (11)$$

Moreover, it should be pointed out that the P adsorption onto aluminum salt slag is a complicated process due to its complex compositions. The P adsorption in a real adsorption system could be far more complicated.

4. Conclusions

Results obtained from this study have provided some meaningful information:

The characterization study indicated that aluminum salt slag is a complex mixture of metallic Al and various oxides and salts. The chemical bondings of aluminum are mainly Al_2O_3 gamma and AlOOH beta diaspore. The maximum adsorption capacity of aluminum salt slag calculated by Langmuir model varied from 2.312 to 3.467 mg P/g when the temperatures ranged from 288 to 308 K. The kinetic and isotherm studies demonstrated that the P adsorption by aluminum salt slag was chemisorption and the powerful activation energy for chemisorption on the surface of aluminum salt slag was generated thanks to its highly heterogeneous system. Both the relatively high pH (12.0) and low pH (3.0) were beneficial to P adsorption. This phenomenon could be explained by the possible adsorption mechanism of ligand exchange. Besides ligand exchange, precipitation should be another mechanism for P adsorption onto aluminum salt slag, which is concluded by the SEM and EDX analysis. Ligand exchange and precipitation have effect on P adsorption simultaneously. It is believed that ligand exchange is shown to be the dominating mechanism and the precipitation reaction played only a marginal role in the P removal process [38].

Additionally, considering its increasing amount, the potential environment pollution and the high disposal costs of the aluminum salt slag concomitantly generated in the secondary aluminum production process, it is necessary to find a solution with high efficiency and low cost to handle this waste. This research here forcefully revealed the possibility for aluminum salt slag to be a potential adsorbent for P removal from wastewater.

Acknowledgments

The authors thank the support by the National Natural Science Foundation of China (41471433), the National Key Technology R&D Program of China (2012BAC06B03), the support by CRSRI Open Research Program (CKWV2013213/KY), and the Central Public interest Scientific Institution Basal Research Fund (2014-37).

References

[1] K. Łukawska-Matuszewska, R.D. Vogt, R.K. Xie, Phosphorus pools and internal loading in a eutrophic lake with gradients in sediment geochemistry created by land use in the watershed, Hydrobiologia 713 (2013) 183–197.
[2] S.C. Ayaz, Ö. Aktaş, N. Findik, L. Akça, Phosphorus removal and effect of adsorbent type in a constructed wetland system, Desalin. Water Treat. 37 (2012) 152–159.
[3] X.J. Wang, S.Q. Xia, L. Chen, J.F. Zhao, N.J. Renault, J.M. Chovelon, Nutrients removal from municipal wastewater by chemical precipitation in a moving bed biofilm reactor, Process Biochem. 41 (2006) 824–828.
[4] S. Tsuneda, T. Ohno, K. Soejima, A. Hirata, Simultaneous nitrogen and phosphorus removal using denitrifying phosphate-accumulating organisms in a sequencing batch reactor, Biochem. Eng. J. 27 (2006) 191–196.

[5] S. Vasudevan, J. Lakshmi, J. Jayaraj, G. Sozhan, Remediation of phosphate-contaminated water by electrocoagulation with aluminium, aluminium alloy and mild steel anodes, J. Hazard. Mater. 164 (2009) 1480–1486.
[6] P.A. Terry, Removal of nitrates and phosphates by ion exchange with hydrotalcite, Environ. Eng. Sci. 26 (2009) 691–696.
[7] W.T. Chen, C.W. Lin, P.K. Shih, W.L. Chang, Adsorption of phosphate into waste oyster shell: thermodynamic parameters and reaction kinetics, Desalin. Water Treat. 47 (2012) 86–95.
[8] S.J. Yang, Y.X. Zhao, R.Z. Chen, C.P. Feng, Z.Y. Zhang, Z.F. Lei, Y.N. Yang, A novel tablet porous material developed as adsorbent for phosphate removal and recycling, J. Colloid Interface Sci. 396 (2013) 197–204.
[9] N. Bellier, F. Chazarenc, Y. Comeau, Phosphorus removal from wastewater by mineral apatite, Water Res. 40 (2006) 2965–2971.
[10] A. Drizo, C.A. Frost, J. Grace, K.A. Smith, Physico-chemical screening of phosphate-removing substrates for use in constructed wetland systems, Water Res. 33 (1999) 3595–3602.
[11] M. Kõiv, C. Vohla, R. Mõtlep, M. Liira, K. Kirsimäe, Ülo Mander, The performance of peat-filled subsurface flow filters treating landfill leachate and municipal wastewater, Ecol. Eng. 35 (2009) 204–212.
[12] K.C. Cheung, T.H. Venkitachalam, Improving phosphate removal of sand infiltration system using alkaline fly ash, Chemosphere 41 (2000) 243–249.
[13] E. Oguz, Removal of phosphate from aqueous solution with blast furnace slag, J. Hazard. Mater. 114 (2004) 131–137.
[14] L. Zeng, X.M. Li, J.D. Liu, Adsorptive removal of phosphate from aqueous solutions using iron oxide tailings, Water Res. 38 (2004) 1318–1326.
[15] J. Mukhopadhyay, Y.V. Ramana, U. Singh, in: H. Kvande (Ed.), Extraction of Value Added Products from Aluminium Dross Material to Achieve Zero Waste, Light Metals 2005, Minerals, Metals & Materials Soc, Warrendale, 2005, pp. 1209–1212.
[16] J.A.S. Tenorio, D.C.R. Espinosa, Effect of salt/oxide interaction on the process of aluminum recycling, J. Light Met. 2 (2002) 89–93.
[17] P.E. Tsakiridis, Aluminium salt slag characterization and utilization—A review, J. Hazard. Mater. 217–218 (2012) 1–10.
[18] W.J. Bruckard, J.T. Woodcock, Recovery of valuable materials from aluminium salt cakes, Int. J. Miner. Process. 93 (2009) 1–5.
[19] X.C. Wei, R.C. Viadero, S. Bhojappa, Phosphorus removal by acid mine drainage sludge from secondary effluents of municipal wastewater treatment plants, Water Res. 42 (2008) 3275–3284.
[20] G.V. Calder, T.D. Stark, Aluminum reactions and problems in municipal solid waste landfills, Pract. Period. Hazard., Toxic, Radioact. Waste Manage. 14 (2010) 258–265.
[21] B. Zhao, J.S. Song, T. Fang, P. Liu, Z. Jiao, H.J. Zhang, Y. Jiang, Hydrothermal method to prepare porous NiO nanosheet, Mater. Lett. 67 (2012) 24–27.
[22] G. Leofanti, M. Padovan, G. Tozzola, B. Venturelli, Surface area and pore texture of catalysts, Catal. Today 41 (1998) 207–219.
[23] J.B. Zhou, S.L. Yang, J.G. Yu, Z. Shu, Novel hollow microspheres of hierarchical zinc-aluminum layered double hydroxides and their enhanced adsorption capacity for phosphate in water, J. Hazard. Mater. 192 (2011) 1114–1121.
[24] M. Zamparas, Y. Deligiannakis, I. Zacharias, Phosphate adsorption from natural waters and evaluation of sediment capping using modified clays, Desalin. Water Treat. 51 (2013) 2895–2902.
[25] H.N. Yoshimura, A.P. Abreu, A.L. Molisani, A.C. de Camargo, J.C.S. Portela, N.E. Narita, Evaluation of aluminum dross waste as raw material for refractories, Ceram. Int. 34 (2008) 581–591.
[26] P.E. Tsakiridis, P. Oustadakis, S. Agatzini-Leonardou, Aluminium recovery during black dross hydrothermal treatment, J. Environ. Chem. Eng. 1 (2013) 23–32.
[27] L. Zhang, W.T. Wu, J.Y. Liu, Q. Zhou, J.H. Luo, J.Q. Zhang, X.Z. Wang, Removal of phosphate from water using raw and activated laterite: batch and column studies, Desalin. Water Treat. 52 (2014) 775–783.
[28] C. Gerente, V.K.C. Lee, P. Cloirec, G. McKay, Application of chitosan for the removal of metals from wastewaters by adsorption—Mechanisms and models review, Crit. Rev. Environ. Sci. Technol. 37 (2007) 41–127.
[29] Y.S. Ho, G. McKay, Sorption of dye from aqueous solution by peat, Chem. Eng. J. 70 (1998) 115–124.
[30] J. Villanueva-Cab, H.X. Wang, G. Oskam, L.M. Peter, Electron diffusion and back reaction in dye-sensitized solar cells: The effect of nonlinear recombination kinetics, J. Phys. Chem. Lett. 1 (2010) 748–751.
[31] Q. Yu, R. Zhang, S. Deng, J. Huang, G. Yu, Sorption of perfluorooctane sulfonate and perfluorooctanoate on activated carbons and resin: Kinetic and isotherm study, Water Res. 43 (2009) 1150–1158.
[32] S.I. Lyubchik, A.I. Lyubchik, O.L. Galushko, L.P. Tikhonova, J. Vital, I.M. Fonseca, S.B. Lyubchik, Kinetics and thermodynamics of the Cr(III) adsorption on the activated carbon from co-mingled wastes, Colloids Surf., A 242 (2004) 151–158.
[33] A. Bhatnagar, E. Kumar, M. Sillanpää, Nitrate removal from water by nano-alumina: Characterization and sorption studies, Chem. Eng. J. 163 (2010) 317–323.
[34] V.C. Srivastava, M.M. Swamy, I.D. Mall, B. Prasad, I.M. Mishra, Adsorptive removal of phenol by bagasse fly ash and activated carbon: Equilibrium, kinetics and thermodynamics, Colloids Surf., A 272 (2006) 89–104.
[35] H. Stach, J. Mugele, J. Jänchen, E. Weiler, Influence of cycle temperatures on the thermochemical heat storage densities in the systems water/microporous and water/mesoporous adsorbents, Adsorption 11 (2005) 393–404.
[36] H.L. Liu, X.F. Sun, C.G. Yin, C. Hu, Removal of phosphate by mesoporous ZrO_2, J. Hazard. Mater. 151 (2008) 616–622.
[37] J. Tofan-Lazar, H.A. Al-Abadleh, Kinetic ATR-FTIR studies on phosphate adsorption on iron(oxyhydr)oxides in the absence and presence of surface arsenic: Molecular-level insights into the ligand exchange mechanism, J. Phys. Chem. A 116 (2012) 10143–10149.
[38] Y.J. Xue, H.B. Hou, S.J. Zhu, Characteristics and mechanisms of phosphate adsorption onto basic oxygen furnace slag, J. Hazard. Mater. 162 (2009) 973–980.